San Jose State University
SJSU ScholarWorks

Faculty Publications

Meteorology and Climate Science

June 2002

Transport Out of the Antarctic Polar Vortex from a Three-dimensional Transport Model

Shuhua Li
NASA Goddard Space Flight Center, Greenbelt, Maryland

Eugene Cordero
San Jose State University, eugene.cordero@sjsu.edu

David J. Karoly
Monash University, Australia

Follow this and additional works at: https://scholarworks.sjsu.edu/meteorology_pub

Part of the Atmospheric Sciences Commons, Climate Commons, and the Meteorology Commons

Recommended Citation

Transport out of the Antarctic polar vortex from a three-dimensional transport model

Shuhua Li,[1] Eugene C. Cordero, and David J. Karoly

School of Mathematical Sciences, Monash University, Australia

[1]   A three-dimensional chemical transport model is utilized to study the transport out of the Antarctic polar vortex during the southern hemisphere spring. On average, over five consecutive years between 1993 and 1997, horizontal transport out of the vortex into the midlatitude stratosphere is smaller than vertical transport into the troposphere. However, there is significant interannual variability in the magnitude of mass exchange, which is related to year-to-year fluctuations in planetary wave activity. In 1994 the net loss of the vortex tracer mass in September is similar to that in October. However, the relative mass flux entering the midlatitude stratosphere and the troposphere differ between the two months. The ratio of horizontal transport out of the vortex to vertical transport into the troposphere is about 3:7 in September and 5:5 in October, indicating the higher permeability of the vortex in October compared to September. The September mass flux into the troposphere is larger than in October, consistent with the fact that stronger diabatic cooling occurs in September than October over Antarctica. The estimated ozone change at southern midlatitudes due to the intrusion of ozone-depleted air from high latitudes during September–October 1994 is about −0.44% per decade, which could contribute up to 10% of observed ozone decline at southern midlatitudes in spring. This amount is an underestimate of the dilution effect from high latitudes during the spring season, as it does not include the vortex breakup in late spring.   *INDEX TERMS:* 3334 Meteorology and Atmospheric Dynamics: Middle atmosphere dynamics (0341, 0342); 0341 Atmospheric Composition and Structure: Middle atmosphere—constituent transport and chemistry (3334); 0342 Atmospheric Composition and Structure: Middle atmosphere—energy deposition; *KEYWORDS:* transport, polar vortex, mass flux, dilution effect

1.   Introduction

[2]   Since the discovery of the Antarctic ozone hole in the middle 1980s [*Farman et al.*, 1985], many observational and modeling studies have attempted to explore the dynamical and chemical aspects responsible for the occurrence of this annual event during southern springtime [*World Meteorological Organization* (*WMO*), 1992, 1995, 1999]. A high degree of dynamical isolation associated with the Antarctic polar vortex maintains a unique environment suitable for ozone depletion involving polar stratospheric clouds (PSCs) [*Solomon*, 1999; *WMO*, 1999]. In recent years a number of studies have explored characteristic mass exchange and transport between the polar vortex and the surrounding regions [*Hartmann et al.*, 1989a, 1989b; *Proffitt et al.*, 1989; *Schoeberl et al.*, 1989, 1992; *Tuck et al.*, 1992; *Bowman*, 1993a; *Tuck et al.*, 1993; *Plumb et al.*, 1994; *Wauben et al.*, 1997]. *Juckes and McIntyre* [1987] and *McIntyre* [1989] argued that the cross-vortex mass exchange

at the vortex edge is inhibited by the sharp potential vorticity (PV) gradients; thus the polar vortex might behave as an isolated material entity. This vortex isolation hypothesis has been supported by a number of numerical modeling studies [*Juckes and McIntyre*, 1987; *Salby et al.*, 1990; *Polvani and Plumb*, 1992; *Bowman*, 1993a; *Norton*, 1994; *Wauben et al.*, 1997].

[3]   *Chen* [1994] and *Chen et al.* [1994] investigated the isentropic transport and mixing across the vortex edge using horizontal winds from the UK Met (UKMO) data assimilation system. They found that there is a transition layer around the 400 K isentropic surface. Above 400 K, there is little mixing between the vortex and midlatitudes, and below 400 K, much more mixing across the vortex edge takes place. *McIntyre* [1995] introduces the idea of a "subvortex" region. The existence of a transition altitude was also verified by trajectory analysis [*Bowman*, 1993b]. The altitude of the transition level varies through the season [*Haynes and Shuckburgh*, 2000]. *Wauben et al.* [1997] investigated the transport of tracers out of the Antarctic vortex in winter and spring, based on averaged transport rates over August–September–October during four consecutive years (1990–1993). The uncertainties arising from wind resolution and the Antarctic tropopause height have been noted in previous work. More importantly, the definition of the vortex edge

---

Table 1. Vertical Levels in Pressure Above 150 hPa Represented by GASP and UKMO Data Sets[a]

GASP	UKMO
150	147
100	100
70	68
46	50
30	32
	22
	15
10	10
	7
	4.6
	3.2
	2.2
	1.5
	1
	0.7
	046
	0.32

[a] Units are hPa.

perhaps has an important impact on the transport magnitude. *Wauben et al.* [1997] assumed 61°S latitude as the edge of the polar vortex. Since the vortex is not always a symmetrically circumpolar system, a latitude circle cannot consistently represent the edge of the evolving vortex [*Tuck and Proffitt*, 1997]. Accordingly, we determine the vortex boundary by steep PV gradients which prove to represent the vortex edge more realistically than a specific latitude.

[4] It is of importance to estimate transport rates between the polar vortex and southern midlatitudes because these exchange rates provide insight into the extent to which ozone-depleted air from the Antarctic polar vortex might impact the ozone levels at midlatitudes. On the basis of three-dimensional (3-D) model simulations driven by two sets of analyzed data, this paper quantifies the transport out of the Antarctic polar vortex during southern spring and examines the interannual variability in the transport rates based on analysis over five consecutive years, 1993–1997. Finally, the midlatitude ozone change due to polar effects is estimated for spring 1994.

2. Model and Specifics of Simulations

2.1. Model Description

[5] The 3-D off-line chemical transport model (CTM) was based on the chemical transport model developed at the National Center for Atmospheric Research (NCAR) by *Rasch and Williamson* [1990] and *Rasch et al.* [1994]. This model has been modified and updated so as to enable the model to be run on the available machines and with different input data sets. To preserve shapes of tracer distribution and minimize numerical diffusion, the model uses a semi-Lagrangian transport scheme [*Williamson and Rasch*, 1989]. To keep global tracer mass constant, a "mass fixer" is used after advection (see *Rasch et al.* [1995] for details). This model has been used for many CTM studies to simulate stratospheric aerosols [*Boville et al.*, 1991], radioactive isotopes [*Rasch et al.*, 1994], CFCs in the troposphere [*Hartley et al.*, 1994], stratospheric species [*Rasch et al.*, 1995], long-lived stratospheric constituents [*Waugh et al.*, 1997], and the springtime breakup of the Antarctic

ozone hole (S. Li et al., Three-dimensional simulations of springtime breakup of the Antarctic ozone hole, submitted to *Australian Meteorological Magazine*, 2001, hereinafter referred to as Li et al., submitted manuscript, 2001).

[6] This model can be run at any reasonable time step and spatial resolution. In other words, the model output only depends on the resolution of driving fields (e.g., wind components and temperature at pressure or σ (σ = P/P_s) coordinates). This facilitates studies with differing resolution, using either general circulation model (GCM) output or assimilated data as driving fields.

2.2. Data and Experiments

[7] Two sets of assimilated data are used here to drive the 3-D CTM. The first data set is from the Global Assimilation and Prediction system (GASP), Australia. As a global forecast system, GASP analyses provide 3-D wind components and many other variables, with specific attention to the Southern Hemisphere [*Bourke et al.*, 1995; *Seaman et al.*, 1995]. The original data for 1994 are of R53 resolution (equivalent to 162 longitudes × 134 latitudes) and 19 σ levels in the vertical (approximately pressures 991 to 10 hPa). They are available every 6 hours, at 0500, 1100, 1700, and 2300 UTC, respectively. For most of the CTM simulations in this study the GASP winds and temperature are truncated to R21 (64 longitudes × 56 latitudes).

[8] The second set of assimilation data is from UARS (Upper Atmosphere Research Satellite) UKMO global analyses [*Swinbank and O'Neill*, 1994], which are available once a day, at 1200 UTC. The data are distributed at 22 pressure levels equally spaced in pressure-altitude (from 1000 up to 0.32 hPa) and converted horizontally from regular 3.75° longitude by 2.5° latitude resolution to R31 (96 longitudes × 80 latitudes). The vertical levels represented by the two data sets in the stratosphere are given in Table 1. As the UKMO data cover the entire stratosphere, they enable examination of transport up to the upper stratosphere and thus make it possible to simulate total column ozone in the atmosphere. In addition, comparisons with descent rates derived from observations [e.g., *Godin et al.*, 2001] in the high-latitude lower stratosphere indicate that UKMO data appear to be more realistic than GASP data.

[9] In order to quantify the transport between the polar vortex and southern midlatitudes, a series of CTM simulations for passive idealized tracers are performed using GASP and UKMO assimilated winds as driving fields. In these model simulations the initial nonzero tracers are initialized at each grid cell inside the polar vortex determined by largest PV gradients and vertically confined in the lower stratosphere between 30 and 100 hPa. The tracer concentration is set to be zero elsewhere. Since no other source/sinks are considered during the model integration, these experiments should enable an examination of 3-D transport properties, with particular emphasis on the polar/midlatitude transport.

3. Transport Out of the Polar Vortex in Spring 1994

3.1. Net Transport Out of the Polar Vortex

[10] The spatial distribution of passive tracers in October 1994 is compared with observed total ozone from Total
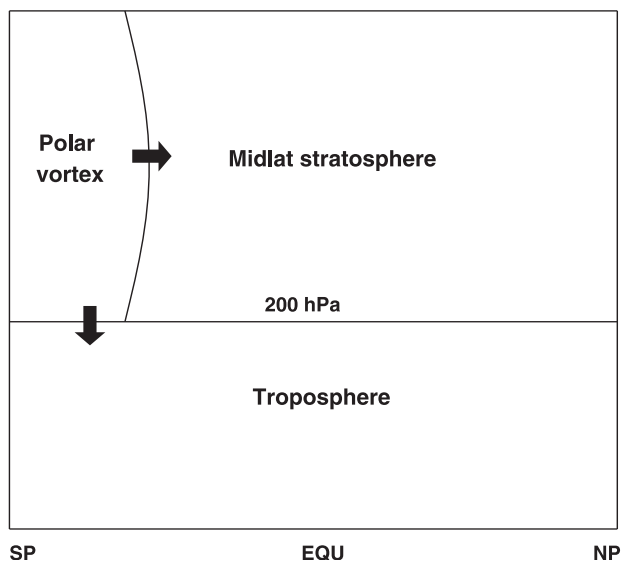
Figure 1. Schematic of three regions of the model atmosphere used to estimate transport rates between different regions, where the polar vortex edge is determined by large PV gradients. The vortex edge is represented as a curve to emphasize that it has a nonconstant latitude with varying altitude.

Ozone Mapping Spectrometer (TOMS). On 1 October the nonzero tracers (100 ppmv) are initialized in each grid cell inside the south polar vortex in the 30–100 hPa layer. The tracer distribution released inside the vortex demonstrates a qualitative agreement with the area extent of low total ozone values, the Antarctic "ozone hole." The evolution of the ozone hole is well represented by the model simulations of passive idealized tracers. There is good correspondence between the sharp gradients of total ozone and tracer mixing ratio at the edge of the polar vortex. It seems that the 3-D CTM is able to realistically simulate the airflow in middle and high latitudes of the stratosphere. A comparison of the model capability in representing the polar vortex depicted by PV distributions will be given by Li et al. (submitted manuscript, 2001).

[11] On the basis of the CTM simulations of idealized tracers released inside the polar vortex, it is possible to estimate the amount of tracers leaving the vortex, either by horizontal mixing across the vortex boundary or by diabatically descending airflow into the troposphere. Similar to the procedure used by *Wauben et al.* [1997], the model atmosphere is divided into three regions as shown in Figure 1: (1) the Antarctic vortex region, which is determined by steep PV gradients, (2) the midlatitude stratosphere, which is the entire stratosphere minus the south polar vortex region, and (3) the troposphere, which is below 200 hPa level. The choice of 200 hPa as the Antarctic tropopause will be discussed further below.

[12] Figure 2a depicts the amount of tracer mass in each of the three regions for October 1994. After release of tracers inside the vortex on 1 October, there appears to be a sharp decrease of tracer mass inside the vortex during the first few days. Also evident is the rapid increase of tracer mass in the midlatitude stratosphere within 3–4 days after the initial release. These phenomena are expected because

there exist very sharp gradients of tracer mass at the beginning between the vortex air and the surroundings. In fact, there is a fairly steady decline in the vortex tracer mass after a week of integration, which corresponds to the steady increases of tracer mass in the midlatitude stratosphere and in the troposphere. Therefore the first 7-day period is not considered in the subsequent calculations.

[13] In order to quantify the rates at which tracers leave the vortex and enter the other two regions, the following power law equations [*Wauben et al.*, 1997] are used to fit the daily evolution of tracer amount over the period 7–31 October:

$$M_V = \alpha^t, \tag{1}$$

$$M_S = f_S(1 - \alpha^t), \tag{2}$$

$$M_T = f_T(1 - \alpha^t), \tag{3}$$

where M_V, M_S, and M_T represent the nondimensional tracer masses (i.e., the actual cumulative tracer masses scaled with the vortex tracer mass at day 7) in the vortex, the
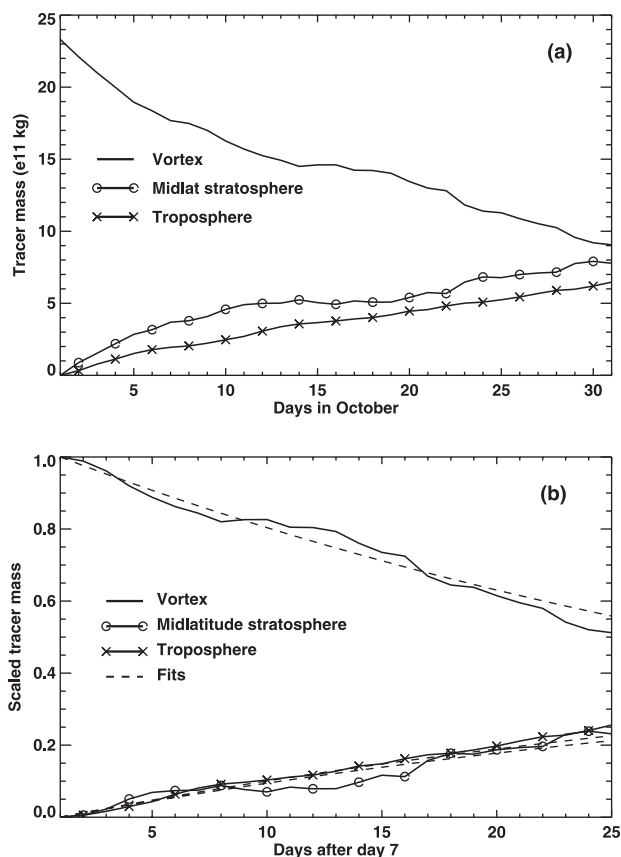

Figure 2. (a) Temporal evolution of the total amount of tracer mass in the stratospheric vortex, the midlatitude stratosphere, and the troposphere in October 1994. (b) Temporal evolution of the scaled tracer mass in the three regions for day 7–31 of October 1994. Dashed lines indicate the power law fits. These calculations were for the CTM with GASP R21 winds.

midlatitude stratosphere, and the troposphere, respectively. The parameter α is the fractional decrease in vortex tracer amount per time increment t (in days), and f_S, f_T are the fractional amounts of tracers entering the midlatitude stratosphere and the troposphere, respectively. For the purpose of mass conservation, f_S and f_T must satisfy

$$f_S + f_T = 1. \qquad (4)$$

Obviously, at the beginning of fitting, $M_V = 1$ and $M_S = M_T = 0$. The parameter α can be determined by fitting equation (1) to the nondimensional tracer mass in the vortex region. This value is then used to fit the relative tracer masses in the other two regions to obtain f_S and f_T according to equations (2) and (3), respectively.

[14] It should be pointed out that the above equations are valid under the following assumptions: (1) during the integration time, tracers do not flow back to the vortex region, and (2) the net tracer flow between the midlatitude stratosphere and the troposphere is negligible [*Wauben et al.*, 1997]. Assumption 1, which is valid before the tracer mass gradient is opposite, is tested by initializing nonzero tracer at midlatitudes only. In this experiment, only a small fraction of tracers flows into the vortex region. According to the fits for October 1994 (Figure 2b), the vortex region loses about 2.38% of its mass per day, ∼48% of which enters the midlatitude stratosphere through quasi-horizontal mixing across the vortex edge, while 52% of the vortex outflow is transported to the troposphere by descending airflow (see Table 2 for details). This implies that the mass flow out of the vortex to the midlatitude stratosphere is nearly identical to that flushing into the troposphere in October 1994.

[15] If the initial nonzero tracer inside the vortex is initialized on 1 September, the temporal evolution of tracer mass in the three regions, particularly in the midlatitude stratosphere and the troposphere, appears to be different from that in October (not shown). The fitted tracer flow rates are significantly different between the two months (Table 2). Although the September total vortex outflow is the same as October, the horizontal transport across the vortex edge in September is substantially weaker than that in October, indicating stronger isolation of the vortex in September compared to October. The percentage of mass flux along with descending airflow to the troposphere becomes higher in September. The approximate ratio of horizontal to vertical transport is about 2:8 in September and 5:5 in October. Note that the tracer flow out of the vortex is twice the size of *Wauben et al.*'s [1997] estimate.

[16] According to *Tuck and Proffitt* [1997] the August-October tropopause over and around Antarctica is near 200 hPa, although this altitude experiences considerable seasonal variation (e.g., the Antarctic tropopause pressure is 300 hPa in summer). In the above analysis the altitude of the Antarctic tropopause, which is also used as the bottom of the vortex, is assumed to be 200 hPa. To test the dependence of tracer flow rates on the choice of this level, the above fitting procedure is repeated for the September simulation with differing altitude of the tropopause. Changing the bottom of the vortex from 200 to 250 hPa decreases the rate of vortex mass loss from 2.39% to 2.11% per day. At the same time, the fractional inflow to the troposphere decreases from 79% to 64%, and the relative transport to

Table 2. Tracer Flow Rate in Three Regions for September and October 1994[a]

	GASP (R21)		UKMO (R31)	
	Sept.	Oct.	Sept.	Oct.
PV-based vortex	−2.39	−2.38	−1.42	−1.57
Midlatitude stratosphere	0.49 (21)	1.15 (48)	0.44 (31)	0.71 (45)
Troposphere	1.90 (79)	1.23 (52)	0.98 (69)	0.86 (55)

[a] Flow rates are in percent per day. Values in parentheses are relative inflow rates (percent of total vortex outflow) in the midlatitude stratosphere and the troposphere.

the midlatitude stratosphere increases. This could have been expected as there is a larger boundary between the polar and midlatitude regions in this case.

[17] It is important to note that the transport across the vortex edge in this study is less episodic than in the study by *Wauben et al.* [1997]. As they noted, part of the episodic events may be caused by intersection of the real vortex boundary with the fictitious boundary at 61°S. Indeed, after using PV gradients to determine the vortex edge the across-vortex transport seems to be relatively steady. Nevertheless, the evolution of the horizontal outflow still displays more episodic events than the vertical transport. This is not surprising because quasi-horizontal mixing across the vortex edge is induced by occasional planetary wave breaking [e.g., *McIntyre*, 1989; *Bowman*, 1993a], while the vertical transport is performed by steady diabatic descent due to radioactive cooling [e.g., *Rosenfield et al.*, 1987, 1994].

[18] The above simulations of idealized tracers are also performed using UKMO assimilated data as driving fields. The initial nonzero tracers are released at the model levels between 30 and 100 hPa inside the PV-based polar vortex. The fitted transport magnitudes for the same periods are listed in Table 2. Compared with GASP-based estimates, the total vortex outflow in September and October 1994 is much smaller. However, the relative transport rates to the midlatitude stratosphere and the troposphere are similar to GASP-based transport rates.

3.2. Sensitivity of Transport to Resolution

[19] In order to test the sensitivity of transport magnitude to changes in resolution, an additional run using higher-resolution (R53) GASP winds has been performed for October 1994. The temporal evolution of the tracer mass in each region is shown in Figure 3, together with the results at R21 resolution. It is evident that the tracer amount in the midlatitude stratosphere experiences little change in response to differing horizontal resolution. However, there is a large increase in the tracer mass flowing to the troposphere corresponding to a finer resolution. It is interesting that there is a bias toward a smaller vortex size in the lower resolution data.

[20] The fitted transport rates in October 1994 are listed in Table 3 for the two GASP resolutions, along with UKMO-based estimate for the same period. While the effect of GASP resolution on the amount of tracers leaving the vortex is relatively small, the tracer mass flowing into the troposphere undergoes substantial change. Using a coarser resolution tends to increase the amount of tracers entering the midlatitude stratosphere but to decrease the tracer
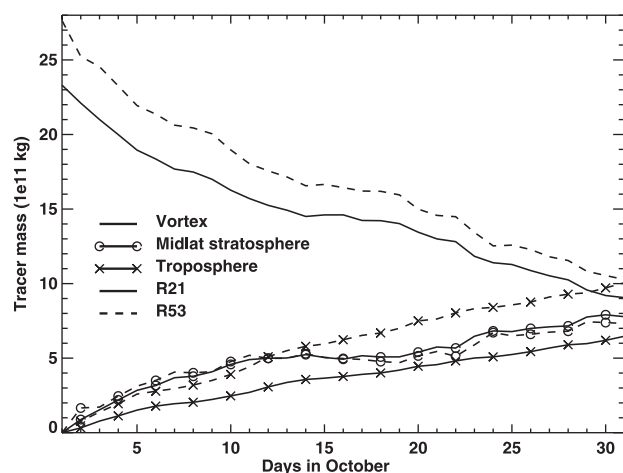
Figure 3. Temporal evolution of the total amount of tracer mass in the stratospheric vortex, the midlatitude stratosphere, and the troposphere in October 1994 for two different GASP resolutions R21 and R53.

Table 3. Tracer Flow Rate in Three Regions for October 1994 Based on CTM Simulations Driven by GASP Winds at Two Different Horizontal Resolutions (R21, R53) and UKMO Data at R31[a]

Horizontal Resolution	PV-Based Vortex	Midlatitude Stratosphere	Troposphere
GASP – R53	−2.71	1.02 (38)	1.69 (62)
UKMO – R31	−1.57	0.71 (45)	0.86 (55)
GASP – R21	−2.38	1.15 (48)	1.23 (52)

[a] Flow rates are in percent per day. Values in parentheses are relative inflow rates of the midlatitude stratosphere and the troposphere in percent of total vortex outflow.

amount descending into the troposphere. This is in general agreement with *Wauben et al.* [1997].

[21] On the basis of the estimated transport using GASP data, when the horizontal resolution changes from R53 to R21, the total vortex outflow decreases by ∼12%; the change in horizontal outflow and the vertical transport is 10%. This indicates relative insensitivity of the transport to resolution at mid-high latitudes, consistent with the results of ozone simulations (Li et al., submitted manuscript, 2001). With a resolution between R21 and R53 the UKMO-based estimates are between GASP R53 and R21 in terms of the relative inflow rates in the midlatitude stratosphere and the troposphere. The change in the transport partitioning is driven by the polar/midlatitude transport change. It has been shown that coarser horizontal resolution corresponds to higher permeability of the polar vortex at the expense of less percentage of vertical transport into the troposphere. Note that assimilated vertical winds tend to have a lot of high-frequency noise which will produce spurious transport. In this case the lower-resolution winds will actually give more accurate results.

[22] From the above analysis the horizontal model resolution has impact on the polar/midlatitude transport, but this effect is smaller than the impact on vertical transport. Further, the results presented here seem to indicate that the horizontal resolution of R21 or R31 is sufficient to provide a reasonable estimate of transport between the polar vortex and southern midlatitudes. It is suggestive that the difference in the transport magnitude out of the polar vortex between GASP and UKMO-based calculations is primarily ascribed to their differences in vertical resolution, especially the vertical coverage of the stratosphere; the effect of differences in horizontal resolution appears to be secondary.

4. Interannual Variability of the Transport

[23] In order to gain insight into the interannual variability of the transport rates, the above simulation and analysis using UKMO data as driving fields are repeated for the years 1993, 1995, 1996, and 1997. On the basis of the magnitude of transport over the 5 consecutive years (1993–1997), there appears to be large interannual variability in total vortex outflow and the partitioning between the tracer flows into the midlatitude stratosphere and the troposphere (Table 4).

[24] On average over the 5 years for the September-October season, the total loss of the vortex mass is 1.37% per day, or ∼55% during the 2 months. The largest portion (72%) of this outflow enters the troposphere through steady descending motions. The total outflow varies from 1.18% per day in 1993 to 1.52% per day in 1994. The relative inflow rates into the midlatitude stratosphere range between 16% and 39%. The year-to-year variability of the transport magnitudes is found to be related to the fluctuations of planetary wave activity from one year to another. As revealed by eddy heat flux $(\overline{v'T'})$ in the lower stratosphere, the Southern Hemisphere seasonal maximum in wave driving is observed in September–October [*Randel and Newman*, 1999]. The eddy heat flux at 100 hPa averaged between 50° and 80°S is listed in Table 4. Apparently, the strength of planetary wave activity is reasonably well correlated with the transport magnitude out of the polar

Table 4. Tracer Flow Rate in Three Regions During September–October Over Five Consecutive Years 1993–1997[a]

	1993	1994	1995	1996	1997	Average
PV-based vortex	−1.18	−1.52	−1.48	−1.25	−1.44	−1.37
Midlatitude stratosphere	0.41 (35)	0.59 (39)	0.44 (30)	0.20 (16)	0.30 (21)	0.39 (28)
Troposphere	0.77 (65)	0.93 (61)	1.04 (70)	1.05 (84)	1.14 (79)	0.98 (72)
$(\overline{v'T'})$, K m/s	−12.8	−19.6	−12.3	−11.2	−11.0	

[a] Flow rates are in percent per day. Values in parentheses are relative inflow rates (percent of total vortex outflow) in the midlatitude stratosphere and the troposphere. The model transport is driven by winds from UKMO assimilation data. The zonal mean eddy heat flux at 100 hPa, averaged over 50–80°S, during September–October for each year is also given.
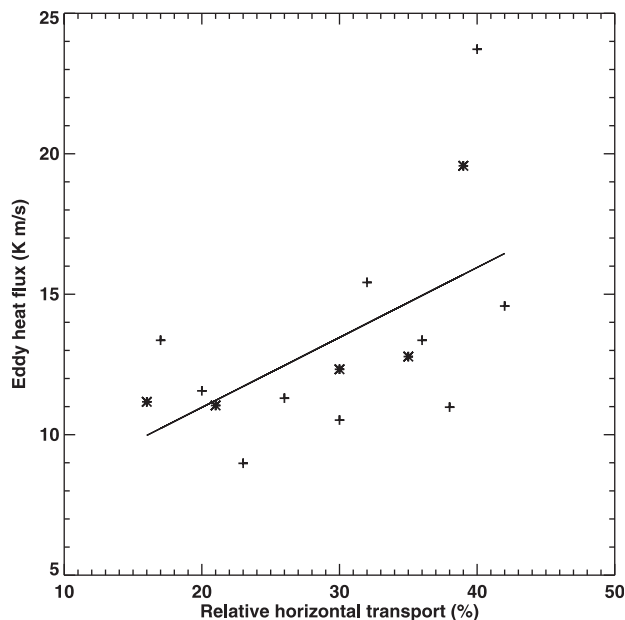
Figure 4. Scatterplots of eddy heat flux $(\overline{v'T'})$ at 100 hPa, over the range 50–80°S, against the relative horizontal transport in percent for September and October over the years 1993–1997. The solid line represents the least squares fit. The 15 points are the 10 individual monthly values (pluses) for September and October 1993–1997, as well as the five bimonthly values (asterisk).

vortex, particularly with the relative horizontal transport rates (in percent of total vortex outflow).

[25] To illustrate the correlation of year-to-year variations between transport magnitude and wave activity, Figure 4 shows the scatterplots of $(\overline{v'T'})$ against relative horizontal transport in percent of total vortex outflow. Their linear correlation coefficient is 0.57. There appears to be evidence that the stronger the wave driving, the larger the relative horizontal transport out of the polar vortex.

5. Midlatitude Ozone Trends Due to Polar Effects

[26] The magnitude of polar/midlatitude transport can be used to estimate changes in midlatitude ozone levels caused by mass flux of ozone-depleted air from the Antarctic polar vortex. In section 4 the tracer flow rates were estimated for three different regions. In order to illustrate the transport rates in individual layers, Table 5 gives the percentage of tracer mass entering the midlatitudes (40–50°S) for September and October 1994, respectively. First, the horizontal mixing in the lower stratosphere is significantly larger than that in the middle stratosphere. There is a gradual increase in mixing rates at lower altitudes, consistent with the results of [*Haynes and Shuckburgh*, 2000]. Second, the horizontal transport in October is always greater than in September in corresponding layers. The estimated transport based on UKMO data as driving fields is much less than GASP-based transport.

[27] We choose 40–50°S to represent midlatitudes for two reasons: (1) this region is away from the polar vortex; and (2) the area in this region is similar in size to the polar cap south of 60°S. On the basis of the percentage of tracer mass flowing into the midlatitudes (40–50°S), it is possible

to estimate how much of the midlatitude ozone change is due to intrusion of ozone-poor air from the Antarctic polar vortex. Assuming the ozone-depleted air from the polar region is mixed horizontally to the midlatitudes, then the vortex air entering the midlatitude stratosphere is given in Table 5 as percentage of initial mass in the corresponding layers. We assume that within the polar vortex the air is well mixed, and the mean ozone profile is obtained from ozone observations. The above transport rates are applied to the ozone profiles averaged in the polar region and midlatitudes, and thus a modified ozone profile for the midlatitudes is obtained. Note that the observed ozone profile at the midlatitudes has suffered "dilution" from ozone-depleted air at high latitudes. Therefore the modified ozone concentration represents ozone values without dilution effect.

[28] Let oz_m and oz_p represent the observed ozone mixing ratio at midlatitudes and polar region, respectively; oz_n represent the modified ozone at midlatitudes; and γ represent the transport rate from high latitudes. Their relationship is expressed by

$$oz_m = (1 - \gamma)oz_n + \gamma oz_p. \tag{5}$$

Then the modified ozone at an individual level can be written as

$$oz_n = \frac{oz_m - \gamma oz_p}{1 - \gamma}. \tag{6}$$

As an example, the mean ozone profiles in October 1994 are shown in Figure 5, where the transport is driven by GASP winds. The changes in column ozone derived from the observed and modified ozone profiles at midlatitudes are then calculated for September and October 1994, respectively.

[29] The changes in column ozone due to this effect, using GASP and UKMO-based transport rates, are listed in Table 6. Because UKMO-based transport is closer to the real atmosphere than GASP-based simulation (Li et al., submitted manuscript, 2001), we focus here on the estimates based on UKMO data as driving fields. According to total ozone observations the Antarctic ozone hole begins to develop in August and breaks up in early December or late November; the Antarctic ozone deficit reaches a maximum in September and October. Therefore the sum of ozone trends in this period accounts for most of the ozone change at southern midlatitudes induced by air intrusion from the Antarctic ozone hole. The consequent decadal ozone trends, as calculated using a single year, are about −0.44% from UKMO-based transport.

Table 5. Percentage of Tracer Mass Flowing Into the Midlatitudes (40–50°S)[a]

Pressure Level, hPa	GASP		UKMO	
	Sept.	Oct.	Sept.	Oct.
30	0.89	3.34	0.19	0.79
50	1.41	4.88	0.40	1.50
70	1.96	5.80	0.65	2.76
100	2.76	5.76	0.80	3.69

[a] On last day of September and October 1994 for individual layers centered at pressure levels as below. Values are percentage of initial mass in the corresponding layers.
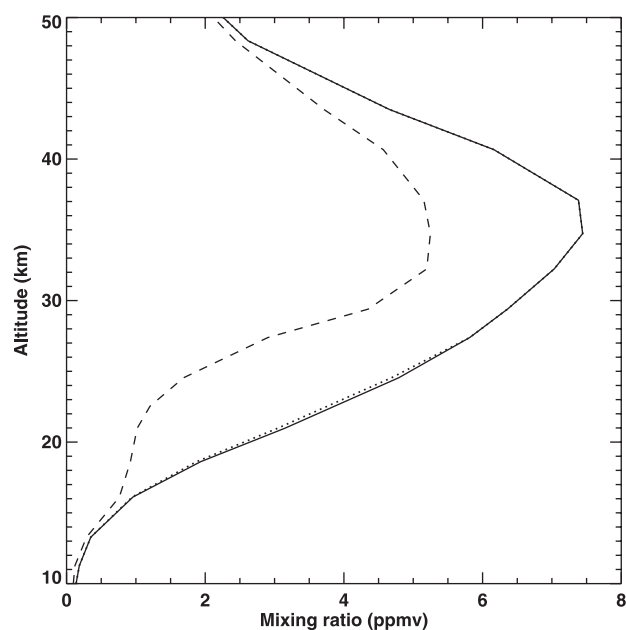
Figure 5. Monthly mean zonally averaged ozone profile for October 1994 in polar region south of 60°S (dashed) and midlatitudes 40–50°S (dotted), and the modified ozone at the midlatitudes without dilution (solid) based on simulations driven by GASP winds.

[30] From ozone observations in the last two decades, the ozone depletion rates at southern midlatitudes (40–50°S) for September–October season are 4–5% per decade [e.g., *Herman et al.*, 1993; *Komhyr et al.*, 1997; *WMO*, 1995, 1999]. According to the estimate based on UKMO winds to drive the transport, only ~10% of the midlatitude ozone trend comes from the air intrusion from the Antarctic polar vortex. Note that the estimate does not include the dilution effect of ozone-depleted air during and after the final breakup of the polar vortex. This amount, therefore, is an underestimate of the dilution effect.

6. Conclusions

[31] In an attempt to quantify the transport out of the south polar vortex, results from a series of CTM simulations of idealized tracers have been used to estimate tracer flow rates for September-October, the season when major ozone depletion occurs. The model atmosphere is simply divided into three parts, i.e., the stratospheric vortex, the midlatitude stratosphere, and the troposphere. On average over 5 consecutive years 1993–1997, the transport out of the vortex flowing into the midlatitude stratosphere is much smaller than that descending to the troposphere, at the ratio of 28:72, suggesting that the vortex is fairly well isolated from its surroundings. However, there is significant interannual variability in the magnitude of transport, which appears to be related to the year-to-year fluctuations of planetary wave activity.

[32] For the case of 1994 the horizontal transport into the midlatitude stratosphere is much weaker than the vertical transport to the troposphere in September, with a ratio of 3:7 from the UKMO-based estimate. However, the partitioning of the vortex outflow differs in October, with ~45% of total

vortex outflow entering the midlatitude stratosphere and 55% to the troposphere. The relative percentage of tracer mass flowing into the midlatitude stratosphere is much lower in September than in October. This reflects the difference in the extent of the vortex isolation from its surroundings between the 2 months. In September the polar vortex is stronger with a higher degree of isolation; while in October, particularly in late October, the vortex becomes gradually weaker and thus exhibits less isolation (or higher permeability) at the vortex boundary compared to September. As a result, the relative transport rate into the midlatitude stratosphere is substantially larger in October than in September.

[33] On the other hand, the relative tracer flow rate descending to the troposphere in September is greater than that in October. This is expected because in September there is stronger diabatic cooling in the polar stratosphere compared to October [*Rosenfield et al.*, 1994]. As a consequence, the descending airflow in September from the stratospheric polar vortex to the troposphere is stronger than in October. Sensitivity study of transport to resolution and data set suggests that differences in transport out of the polar vortex are largely attributed to their difference in vertical resolution and vertical coverage of the stratosphere. However, this cannot be strictly verified, since spatial and temporal variations in the vertical velocity fields may also be important. Although the magnitude of the transport out of the vortex depends on data sets and their resolution, the partitioning between the horizontal transport into the midlatitude stratosphere and the vertical transport into the troposphere varies little. For instance, the difference is only 3% between GASP R21 and UKMO R31.

[34] The tracer flow rates between the polar vortex and midlatitudes at individual levels are utilized to estimate the effect of Antarctic ozone depletion on ozone levels at southern midlatitudes. In terms of transport rates based on UKMO data as driving fields, the estimated ozone trend at midlatitudes during September–October is about −0.44% per decade due to the dilution effect from ozone-depleted air at high latitudes. This contributes up to 10% of observed ozone decline at southern midlatitudes during September–October period (4–5% per decade). One weakness in this technique for estimating the dilution effect is that we assume the air within the vortex is well mixed; this may cover the vortex edge where much less mixing takes place [*Lee et al.*, 2001].

[35] As a first attempt, we have estimated the Southern Hemisphere midlatitude ozone change due to polar effects before the Antarctic ozone hole breaks up in spring 1994. The estimate does not take into account the dilution effect of ozone-depleted air after the breakup of the Antarctic polar vortex. An important and outstanding issue for further investigation is to examine the effect on midlatitude ozone trends during and after the final breakup of the Antarctic ozone hole.

Table 6. Changes in Ozone Amount at Southern Midlatitudes (40–50°S) Due to Transport of the Antarctic Ozone-Depleted Air for September and October 1994[a]

	Sept.	Oct.	Sum	Trend, %/decade
GASP	−0.32	−1.26	−1.58	−1.32
UKMO	−0.09	−0.44	−0.53	−0.44

[a] In percent of total column ozone.

References

Bourke, W., T. Hart, P. Steinle, R. Seaman, G. Embery, M. Naughton, and L. Rikus, Evolution of the Bureau of Meteorology Global Assimilation and Prediction system, part 2, Resolution enhancements and case studies, *Aust. Meteorol. Mag.*, 44, 19–40, 1995.

Boville, B. A., J. R. Holton, and P. W. Mote, Simulation of the Pinatubo aerosol cloud in a general circulation model, *Geophys. Res. Lett.*, 18, 2281–2284, 1991.

Bowman, K. P., Barotropic simulation of large-scale mixing in the Antarctic polar vortex, *J. Atmos. Sci.*, 50, 2901–2914, 1993a.

Bowman, K. P., Large-scale isentropic mixing properties of the Antarctic polar vortex from analysed winds, *J. Geophys. Res.*, 98, 23,013–23,027, 1993b.

Chen, P., The permeability of the Antarctic vortex edge, *J. Geophys. Res.*, 99, 20,563–20,571, 1994.

Chen, P., J. R. Holton, A. O'Neill, and R. Swinbank, Quasi-horizontal transport and mixing in the Antarctic stratosphere, *J. Geophys. Res.*, 99, 16,851–16,866, 1994.

Farman, J. C., B. G. Gardiner, and J. D. Shanklin, Large losses of total ozone in Antarctica reveal seasonal CLO_x/NO_x interaction, *Nature*, 315, 207–210, 1985.

Godin, S., V. Bergeret, S. Bekki, C. David, and G. Megie, Study of the interannual ozone loss and the permeability of the Antarctic polar vortex from aerosol and ozone lidar measurements in Dumont d'Urville (66.4°S, 140°E), *J. Geophys. Res.*, 106, 1311–1330, 2001.

Hartley, D. E., D. L. Williamson, P. J. Rasch, and R. Prinn, Examination of tracer transport in the NCAR CCM2 by comparison of $CFCl_3$ simulations with ALE/GAGE observations, *J. Geophys. Res.*, 99, 12,855–12,896, 1994.

Hartmann, D. L., K. R. Chan, B. L. Gary, M. R. Schoeberl, P. A. Newman, R. L. Martin, M. Loewenstein, J. R. Podolske, and S. E. Strahan, Potential vorticity and mixing in the south polar vortex during spring, *J. Geophys. Res.*, 94, 11,625–11,640, 1989a.

Hartmann, D. L., L. E. Heidt, M. Loewenstein, J. R. Podolske, J. Vedder, W. L. Starr, and S. E. Strahan, Transport into the South Polar vortex in early spring, *J. Geophys. Res.*, 94, 16,779–16,795, 1989b.

Haynes, P. H., and E. F. Shuckburgh, Effective diffusivity as a diagnostic of atmospheric transport, 2, Troposphere and lower stratosphere, *J. Geophys. Res.*, 105, 22,795–22,810, 2000.

Herman, J. R., R. McPeters, and D. Larko, Ozone depletion at northern and southern latitudes derived from January 1979 to December 1991 Total Ozone Mapping Spectrometer data, *J. Geophys. Res.*, 98, 12,783–12,793, 1993.

Juckes, M. N., and M. E. McIntyre, A high resolution, one-layer model of breaking planetary waves in the stratosphere, *Nature*, 328, 590–596, 1987.

Komhyr, W. D., G. C. Reinsel, R. D. Evans, D. M. Quincy, R. D. Grass, and R. K. Leonard, Total ozone trends at sixteen NOAA/CMDL and cooperative Dobson spectrophotometer observatories during 1979–1996, *Geophys Res. Lett.*, 24, 3225–3228, 1997.

Lee, A., H. Roscoe, A. Jones, P. Haynes, E. Shuckburg, M. Morrey, and H. Pumphrey, The impact of the mixing properties within the Antarctic stratospheric vortex on ozone loss in spring, *J. Geophys. Res.*, 106, 3203–3211, 2001.

McIntyre, M. E., On the Antarctic ozone hole, *J. Atmos. Terr. Phys.*, 51, 29–43, 1989.

McIntyre, M. E., The stratospheric polar vortex and sub-vortex: Fluid dynamics and midlatitude ozone loss, *Philos. Trans. R. Soc. London*, 352, 227–240, 1995.

Norton, W. A., Breaking Rossby waves in a model stratosphere diagnosed by a vortex-following coordinate system and a technique for advecting material contours, *J. Atmos. Sci.*, 51, 654–673, 1994.

Plumb, R. A., D. W. Waugh, R. J. Atkinson, P. A. Newman, L. R. Lait, M. R. Schoeberl, E. V. Browell, A. J. Simmons, and M. Loewenstein, Intrusions into the lower stratospheric Arctic vortex during the winter of 1991–1992, *J. Geophys. Res.*, 99, 1089–1105, 1994.

Polvani, L. M., and R. A. Plumb, Rossby wave breaking, microbreaking, filamentation and secondary vortex formation: The dynamics of a perturbed vortex, *J. Atmos. Sci.*, 49, 462–476, 1992.

Proffitt, M. H., K. K. Kelly, J. A. Powell, B. L. Gary, M. Loewenstein, J. R. Podolske, S. E. Strahan, and K. R. Chan, Evidence for diabatic cooling and poleward transport within and around the 1987 Antarctic ozone hole, *J. Geophys. Res.*, 94, 16,797–16,813, 1989.

Randel, W. J., and P. A. Newman, The stratosphere in the Southern Hemisphere, in *Meteorology of the Southern Hemisphere, Meteorol. Monogr. Ser.*, vol. 27, edited by D. J. Karoly and D. G. Vincent, pp. 243–282, Am. Meteorol. Soc., Boston, Mass, 1999.

Rasch, P. J., and D. L. Williamson, On shape-preserving interpolation and semi-Lagrangian transport, *SIAM J. Sci. Stat. Comput.*, 11, 656–687, 1990.

Rasch, P. J., X. Tie, B. A. Boville, and D. L. Williamson, A three-dimensional transport model for the middle atmosphere, *J. Geophys. Res.*, 99, 999–1017, 1994.

Rasch, P. J., B. A. Boville, and G. P. Brasseur, A three-dimensional general circulation model with coupled chemistry for the middle atmosphere, *J. Geophys. Res.*, 100, 9041–9071, 1995.

Rosenfield, J. E., M. R. Schoeberl, and M. A. Geller, A computation of the stratospheric diabatic circulation using an accurate radiative transfer model, *J. Atmos. Sci.*, 44, 859–876, 1987.

Rosenfield, J. E., and P. A. Newman, and M. R. Schoeberl, Computations of diabatic descent in the stratospheric polar vortex, *J. Geophys. Res.*, 99, 16,677–16,689, 1994.

Salby, M. L., R. R. Garcia, D. O'Sullivan, and J. Tribbia, Global transport calculations with an equivalent barotropic system, *J. Atmos. Sci.*, 47, 1179–1203, 1990.

Schoeberl, M. R., L. R. Lait, P. A. Newman, R. L. Martin, M. H. Proffitt, D. L. Hartmann, M. Loewenstein, J. Podolske, S. E. Strahan, J. Anderson, K. R. Chan, and B. Gary, Reconstruction of the constituent distribution and trends in the Antarctic polar vortex from ER-2 flight observations, *J. Geophys. Res.*, 94, 16,815–16,845, 1989.

Schoeberl, M. R., L. R. Lait, P. A. Newman, and J. E. Rosenfield, The structure of the polar vortex, *J. Geophys. Res.*, 97, 7859–7882, 1992.

Seaman, R., W. Bourke, P. Steinle, T. Hart, G. Embery, M. Naughton, and L. Rikus, Evolution of the Bureau of Meteorology's Global Assimilation and Prediction system, Part 1: Analysis and initialisation, *Aust. Met. Mag.*, 44, 1–18, 1995.

Solomon, S., Stratospheric ozone depletion: A review of concepts and history, *Rev. Geophys.*, 37, 275–316, 1999.

Swinbank, R., and A. O'Neill, A stratosphere-troposphere data assimilation system, *Mon. Weather Rev.*, 122, 686–702, 1994.

Tuck, A. F., and M. H. Proffitt, Comment on "On magnitude of transport out of the Antarctic polar vortex" by Wiel M. F. Wauben et al., *J. Geophys. Res.*, 102, 28,215–28,218, 1997.

Tuck, A. F., T. Davis, S. J. Hovde, M. Noguer-Alba, D. W. Fahey, S. R. Kava, K. K. Kelly, D. M. Murphy, M. H. Proffitt, J. J. Margitan, M. Loewenstein, J. R. Podolske, S. E. Strahan, and K. R. Chan, Polar stratospheric cloud processed air and potential vorticity in the Northern Hemisphere lower stratosphere at midlatitudes during winter, *J. Geophys. Res.*, 97, 7883–7904, 1992.

Tuck, A. F., J. M. Russel III, and J. E. Harries, Stratospheric dryness: Antiphased desiccation over Micronesia and Antarctica, *Geophys. Res. Lett.*, 20, 1227–1230, 1993.

Wauben, W. M. F., R. Bintanja, P. F. J. van Velthoven, and H. M. Kelder, On the magnitude of transport out of the Antarctic polar vortex, *J. Geophys. Res.*, 102, 1229–1238, 1997.

Waugh, D. W., et al., Three-dimensional simulations of long-lived tracers using winds from MACCM2, *J. Geophys. Res.*, 102, 21,493–21,513, 1997.

Williamson, D. L., and P. J. Rasch, Two-dimensional semi-Lagrangian transport with shape preserving interpolation, *Mon. Weather Rev.*, 117, 102–129, 1989.

World Meteorological Organization (WMO), *Scientific Assessment of Ozone Depletion: 1991*, report, Global Ozone Res. and Monit. Proj., Geneva, 1992.

World Meteorological Organization (WMO), *Scientific Assessment of Ozone Depletion: 1994*, report, Global Ozone Res. and Monit. Proj., Geneva, 1995.

World Meteorological Organization (WMO), *Scientific Assessment of Ozone Depletion: 1998*, report, Global Ozone Res. and Monit. Proj., Geneva, 1999.

E. C. Cordero and D. J. Karoly, School of Mathematical Sciences, Monash University, P.O. Box 28M, Clayton, Victoria 3800, Australia. (david.karoly@sci.monash.edu.au)

S. Li, Code 910.4, NASA Goddard Space Flight Center, Greenbelt, MD 20771, USA. (sli@dao.gsfc.nasa.gov)